Cyclooxygenase-2 Inhibitors. 1,5-Diarylpyrrol-3-acetic Esters with Enhanced Inhibitory Activity toward Cyclooxygenase-2 and Improved Cyclooxygenase-2/Cyclooxygenase-1 Selectivity

Mariangela Biava,*[,†] Giulio Cesare Porretta,[†] Giovanna Poce,[†] Sibilla Supino,[†] Stefano Forli,[‡] Michele Rovini,[‡] Andrea Cappelli,[‡,§] Fabrizio Manetti,*[,‡] Maurizio Botta,[‡] Lidia Sautebin,[||] Antonietta Rossi,[||,⊥] Carlo Pergola,[||] Carla Ghelardini,[#] Elisa Vivoli,[#] Francesco Makovec,[○] Paola Anzellotti,[⊗] Paola Patrignani,[⊗] and Maurizio Anzini[‡,§]

Dipartimento di Studi di Chimica e Tecnologia delle Sostanze Biologicamente Attive, Università "La Sapienza", piazzale Aldo Moro 5, I-00185 Roma, Italy, Dipartimento Farmaco Chimico Tecnologico, Università degli Studi di Siena, Via Alcide de Gasperi 2, I-53100 Siena, Italy, European Research Centre for Drug Discovery and Development, via Banchi di Sotto 55, I-53100 Siena, Italy, Dipartimento di Farmacologia Sperimentale, Università di Napoli "Federico II", via D. Montesano 49, I-80131 Napoli, Italy, IRCCS Centro Neurolesi "Bonino-Pulejo", Via Provinciale Palermo - C.da Casazza, I-98124 Messina, Italy, Dipartimento di Farmacologia, Università di Firenze, viale G. Pieraccini 6, I-50139 Firenze, Italy, Rottapharm S.p.A., via Valosa di Sopra 7, I-20052 Monza, Italy, and Department of Medicine and Center of Excellence on Aging, "G. d'Annunzio" University and CeSI, Via dei Vestini 31, I-66013 Chieti, Italy

Received June 26, 2007

The important role of cyclooxygenase-2 (COX-2) in the pathogenesis of inflammation and side effect limitations of current COX-2 inhibitor drugs illustrates a need for the design of new compounds based on alternative structural templates. We previously reported a set of substituted 1,5-diarylpyrrole derivatives, along with their inhibitory activity toward COX enzymes. Several compounds proved to be highly selective COX-2 inhibitors and their affinity data were rationalized through docking simulations. In this paper, we describe the synthesis of new 1,5-diarylpyrrole derivatives that were assayed for their in vitro inhibitory effects toward COX isozymes. Among them, the ethyl-2-methyl−5-[4-(methylsulfonyl)phenyl]-1-[3-fluorophenyl]-1*H*-pyrrol-3-acetate (**1d**), which was the most potent and COX-2 selective compound, also showed a very interesting in vivo anti-inflammatory and analgesic activity, laying the foundations for developing new lead compounds that could be effective agents in the armamentarium for the management of inflammation and pain.

Introduction

Nonsteroidal anti-inflammatory drugs (NSAIDs) represent the standard therapy for the management of inflammation and pain. Although all available NSAIDs are ineffective against disease progression, they show similar antipyretic, anti-inflammatory, and analgesic effects and prove, in particular, to be useful in the treatment of rheumatoid arthritis and osteoarthritis.[1] NSAIDs indiscriminately inhibit both isoforms of cyclooxygenases (COX; constitutive COX-1, responsible for cytoprotective effects and inducible COX-2, responsible for inflammatory effects) with the consequence that they are usually associated with well-known side effects at the gastrointestinal level (mucosal damage, bleeding) and, less frequently, at the renal level.[2] Recent studies have shown that selective COX-2 inhibitors are devoid of the undesirable effects associated with classical, nonselective NSAIDs,[3] and they can also induce apoptosis in colon, stomach, prostate, and breast cancer cell lines.[4] Among them, celecoxib (**3**, Chart 1),[5] rofecoxib (**4**),[6] valdecoxib (**5**),[7] and etoricoxib (**6**)[8,9] have been clinically validated as anti-inflammatory therapeutics for indications such as rheumatoid arthritis. Most of them are characterized by a 1,2-diaryl substitution on a central heterocyclic or carbocyclic ring system. Structure−activity relationship (SAR) studies have shown that a SO_2Me or SO_2NH_2 substituent at the para position of one of the aryl rings often provides optimum COX-2 selectivity and inhibitory potency.[10] Unfortunately, these compounds are associated with well-known adverse cardiovascular effects, such as myocardial infarction.[11−13] The most plausible explanation for this effect is the suppression of COX-2-dependent prostacyclin, which constrains endogenous mediators of platelet activation, hypertension, atherogenesis, and cardiac dysfunction.[14] Moreover, it must be considered that a clinical or genetic predisposition to thrombosis would favor the emergence of a drug-related cardiovascular event.[15] The general impression, as suggested by Fries,[16] is that the efficacy and safety of these drugs is related to multiple factors, such as the chemical properties of the drug (i.e., the selectivity toward COX-2) and individual factors that modulate drug response.[16] Marked intersubject variability in the response (both therapeutic and unwanted) to NSAIDs selective for COX-2 and traditional NSAIDs illustrates a need for the development of novel COX inhibitors that provide an appropriate treatment option for each individual patient.

In this context, we recently reported several investigations describing the design, synthesis, and anti-inflammatory properties of a class of novel pyrrole-containing anti-inflammatory agents. We focused our attention on the synthesis of 1,5-diarylpyrrol-3-acetic and -glyoxylic acid and esters (**7**, Chart 1) as new COX-2 selective inhibitors in which the pyrroleacetic and vicinal diaryl heterocyclic moieties[17] were reminiscent both of indomethacin (**8**) and of the above-cited "coxib" family, respectively. Biological evaluation of compounds **7** showed that insertion of the acetic moiety in the coxib-like scaffold gives rise to very potent and selective COX-2 inhibitors. Among them, several 3-pyrroleacetic esters had very interesting biological

* To whom correspondence should be addressed. Phone: +39 06 4991 3812 (M.B.); +39 0577 234330 (F.M.). Fax: +39 06 4991 3133 (M.B.); +39 0577 234333 (F.M). E-mail: mariangela.biava@uniroma1.it (M.B.); manettif@unisi.it (F.M.).
† Università "La Sapienza".
‡ Università degli Studi di Siena.
§ European Research Centre for Drug Discovery and Development.
|| Università di Napoli "Federico II".
⊥ IRCCS Centro Neurolesi "Bonino-Pulejo".
Università di Firenze.
○ Rottapharm S.p.A.
⊗ "G. d'Annunzio" University and CeSI.

10.1021/jm0707525 CCC: $37.00
Published on Web 10/04/2007 PAGE EST: 8.7

Chart 1. Chemical Structure of Current Inhibitors of COX-2

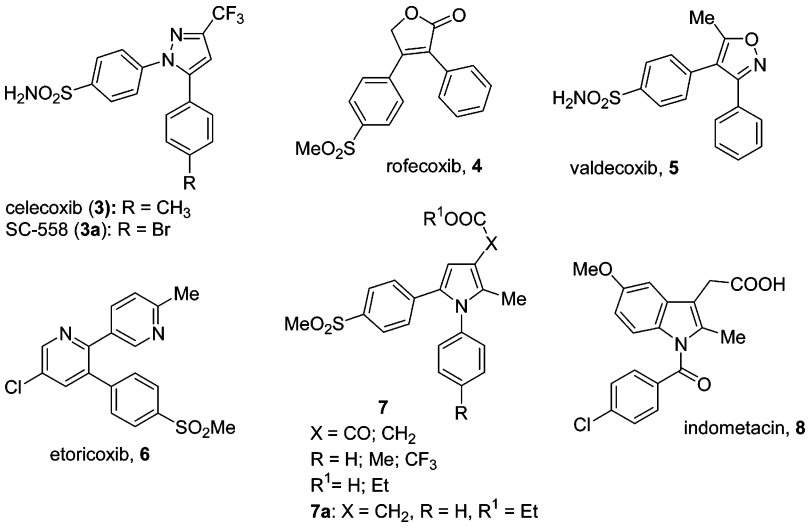

Scheme 1[a]

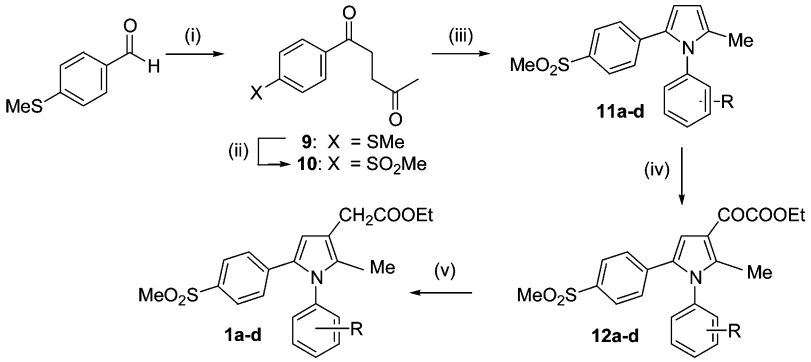

[a] Compounds: **1a**: R = 4-F, 71% yield; **1b**: R = 3,4-F_2, 60% yield; **1c**: R = 4-OMe, 30% yield; **1d**: R = 3-F, 30% yield; **11a**: R = 4-F; **11b**: R = 3,4-F_2; **11c**: R = 4-OMe; **11d**: R = 3-F; **12a**: R = 4-F, 82% yield; **12b**: R = 3,4-F_2, 77% yield; **12c**: R = 4-OMe, 75% yield; **12d**: R = 3-F, 57% yield. Reagents and conditions: (i) CH_2=CHCOMe, NEt_3, EtOH, 75−80 °C, 20 h, thiazolium; (ii) oxone, MeOH/H_2O, rt, 2 h; (iii) $RPhNH_2$, $TiCl_4$, toluene, reflux, 10 h; (iv) EtOCOCOCl, pyridine, CH_2Cl_2, 0 °C, 4 h; (v) Et_3SiH, CF_3COOH, rt, 24 h.

activity profiles, and, in particular, the hit compound (**7a**, Chart 1) exhibited excellent in vitro inhibitory potency toward COX-2, being more active and selective than celecoxib. Such compounds were submitted to a two-step computational protocol consisting of molecular docking calculations and structural optimization of the corresponding complexes. Results led us to hypothesize a binding mode for the pyrrole derivatives able to account for their major SARs. Moreover, theoretical simulations suggested structural modifications of the studied compounds to obtain new derivatives with higher affinity toward COX-2. Accordingly, in the present study, we report the synthesis of compounds **1a**−**d**, **2a**−**f**, **12a**−**d**, and **16a**−**f**, along with their COX (COX-1 and COX-2) inhibiting properties and their rationalization through docking simulations. Compound **1d**, with the best biological profile in terms of affinity and selectivity toward COX-2, as well as percent inhibition of the enzyme (cell culture assay), was also investigated for its in vivo anti-inflammatory and analgesic activity. Moreover, the selectivity of this compound was also determined by the human whole blood (HWB) in vitro assay, which assesses the pattern of relative inhibition for human blood COX-1 and COX-2.

Chemistry

The synthesis of the target compounds is described in Schemes 1 and 2. Briefly, the reaction of 4-methylthiobenzaldehyde with methyl vinyl ketone, according to the Stetter conditions,[18] was very versatile and high yielding in the preparation of the 1,4-diketone **9**, which was transformed into the corresponding 4-methylsulfonyl derivative **10** by means of oxone oxidation.[19] Compound **10**, heated in the presence of the appropriate arylamine, according to the usual Paal−Knoor (thermal) condensation, cyclized after a prolonged reflux to yield the expected 3-unsubstituted 1,5-diarylpyrroles **11a**−**d** in satisfactory yield. The construction of the acetic acid chain was achieved by regioselective acylation[20] of **11a**−**d** with ethoxalyl chloride in the presence of pyridine to give derivatives **12a**−**d**, that were in turn reduced by means of triethylsilane in trifluoroacetic acid[21] to give pyrroleacetic esters **1a**−**d**.

In a similar way, compounds **2a**−**f** were prepared starting from the appropriate benzaldehyde (**13a**−**f**), which was reacted with methyl vinyl ketone, according to the Stetter conditions, to give intermediates **14a**−**f**. They were in turn heated in the presence of 4-methylsulfonylaniline (obtained by H_2O_2 oxidation[22] of the corresponding 4-methylthioaniline), according to the usual Paal−Knoor (thermal) condensation, to give, after a prolonged reflux, the expected 3-unsubstituted 1,5-diarylpyrroles **15a**−**f** in satisfactory yield. The construction of the acetic acid side chain and its subsequent reduction were achieved following the same method described above for compounds **1a**−**f**, thus leading to **16a**−**f** and **2a**−**f**, respectively.

Scheme 2[a]

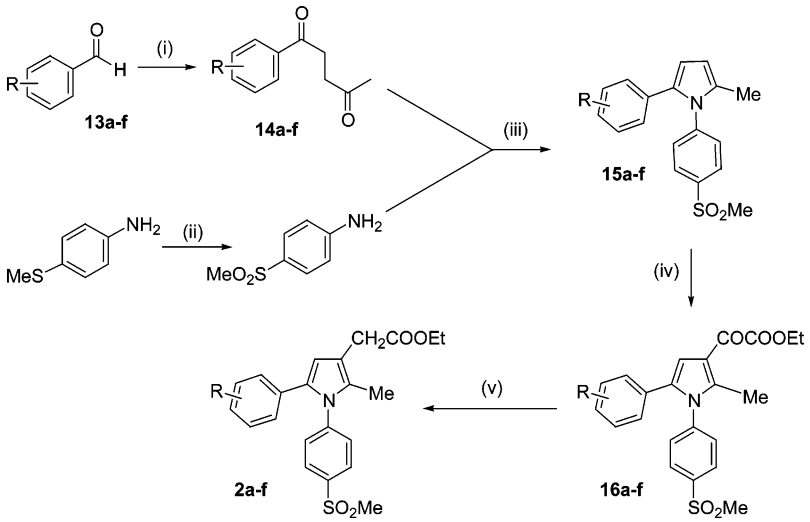

[a] Compounds. **2a**: R = 4-F, 65% yield; **2b**: R = 3,4-F_2, 65% yield; **2c**: R = 4-OMe, 65% yield; **2d**: R = H, 65% yield; **2e**: R = 4-Me, 50% yield; **2f**: R = 4-CF_3, 65% yield; **13a**: R = 4-F; **13b**: R = 3,4-F_2; **13c**: R = 4-OMe; **13d**: R = H; **13e**: R = 4-Me; **13f**: R = 4-CF_3; **14a**: R = 4-F; **14b**: R = 3,4-F_2; **14c**: R = 4-OMe; **14d**: R - H; **14e**: R = 4-Me; **14f**: R = 4-CF_3; **15a**: R = 4-F; **15b**: R = 3,4-F_2; **15c**: R = 4-OMe; **15d**: R = H; **15e**: R = 4-Me; **15f**: R = 4-CF_3; **16a**: R = 4-F, 75% yield; **16b**: R = 3,4-F_2, 80% yield; **16c**: R = 4-OMe, 70% yield; **16d**: R = H, 72% yield; **16e**: R = 4-Me, 74% yield; **16f**: R = 4-CF_3, 70% yield. Reagents and conditions: (i) CH_2=CHCOMe, NEt_3, EtOH, 75−80 °C, 20 h, thiazolium; (ii) H_2O_2/Na_2WO_4, CH_3COOH/H_2O, rt, 1.5 h; (iii) *p*-MeO_2SPhNH_2, $TiCl_4$, toluene, reflux, 10 h; (iv) EtOCOCOCl, pyridine, CH_2Cl_2, 0 °C, 4 h; (v) Et_3SiH, CF_3COOH, rt, 24 h.

Biology

Compounds **1a**−**d**, **2a**−**f**, **12a**−**d**, and **16a**−**f** were all evaluated for their anti-inflammatory activity toward both COX-2 and COX-1 enzymes.

To evaluate COX-1 activity, cells were pretreated with a reference standard (celecoxib) or the test compound (0.01−10 μM) for 15 min and further incubated at 37 °C for 30 min with 15 μM arachidonic acid in order to activate the constitutive COX. At the end of the incubation, the supernatants were collected for the measurement of prostaglandin E_2 (PGE_2) levels by radioimmunoassay. On the other hand, to evaluate COX-2 activity, cells were stimulated for 24 h with *E. coli* lipopolysaccharide (LPS, 10 μg/mL) to induce COX-2, in the absence or presence of test compounds, at the concentrations previously reported. The supernatants were collected for the measurement of PGE_2 by radioimmunoassay. Throughout the time the experiments lasted, triplicate wells were used for the various conditions of treatment. Results are expressed as the mean, for three experiments, of the percent inhibition of PGE_2 production by test compounds with respect to control samples.

Compound **1d** was also evaluated for COX-1 versus COX-2 selectivity by the use of the HWB assay. To evaluate COX-2 activity, 1 mL aliquots of peripheral venous blood samples were incubated in the presence of LPS (10 μg/mL) or saline for 24 h at 37 °C, as previously described.[23] As an index of LPS-induced monocyte COX-2 activity, PGE_2 plasma levels were measured by RIA.[23] COX-1 assay was performed on peripheral venous blood samples drawn from the same donors when they had not taken any NSAID during the two weeks preceding the study. Whole blood TXB_2 production was measured, by RIA, as a reflection of maximally stimulated platelet COX-1 activity in response to endogenously formed thrombin.[24]

Celecoxib and compound **1d** were tested at the final concentrations of 0.01−100 μM in both COX-2 and COX-1 assay.

Moreover, in vivo anti-inflammatory activity of **1d** was also assessed. Male Swiss albino mice (23−25 g) and Sprague−Dawley or Wistar rats (150−200 g) were used. The animals were fed with a standard laboratory diet and tap water ad libitum and kept at 23 ± 1 °C, with a 12 h light/dark cycle, light on at 7 a.m. The paw pressure test was performed, inducing an inflammatory process in the administering i.p. carrageenan 4 h before the test. The carrageenan-induced paw edema test was also performed, evaluating the paw volume of the right hind paw 5 h after the injection of carrageenan and comparing it with saline/carrageenan-treated controls. The analgesic activity of **1d** was also assessed by performing the abdominal constriction test, using mice injected i.p. with a 0.6% solution of acetic acid (10 mL/kg). The number of stretching movements was counted for 10 min, starting 5 min after acetic acid injection.

Results and Discussion

Ester (**1a**−**d** and **2a**−**f**) and α-ketoester (**12a**−**d** and **16a**−**f**) derivatives were synthesized to obtain new compounds more active than **7a** (Chart 1), previously described.[17] Therefore, in the attempt to determine the combined effects of positional, steric, and electronic properties of the substituents on either COX-1 and COX-2 inhibitory potency or COX isozyme selectivity, different substituents were introduced at the pyrrole N1 phenyl ring (such as 3-F, 4-F, 3,4-F_2, and 4-OCH_3), while keeping unchanged the 4-SO_2CH_3 group at the C5 phenyl ring (as in **1a**−**d** and **12a**−**d**). The corresponding regioisomers **2a**−**f** and **16a**−**f** were also synthesized by introducing phenyl, 4-CH_3-phenyl, 4-CF_3-phenyl, 4-F-phenyl, 3-F-phenyl, 3,4-F_2-phenyl, and 4-OCH_3-phenyl substituents at the pyrrole C5 and maintaining the 4-SO_2CH_3-phenyl substituent at N1.

Biological data and SAR analysis confirmed the dependence of the activity on the nature and the mutual position of the substituents on both the phenyl rings at C5 and N1 of the pyrrole ring. In detail, according to our previous results,[17] ester derivatives **1a**−**d** were more active toward COX-2 than the corresponding α-ketoesters **12a**−**d** (0.010 μM, 0.020 μM, 0.026 μM, and 0.010 μM versus 11 μM, 8.4 μM, 0.94 μM, and 0.90 μM, respectively, Table 1). Moreover, COX-1/COX-2 selectivity was much higher than that found for compounds **12a**−**d**. Compounds **2a**−**c** and **2e** showed a micromolar activity toward

Table 1. In Vitro Inhibition (J774 Murine Macrophage Assay) of COX-1 and COX-2 by Compounds **1a**−**d**, **2a**−**f**, **12a**−**d**, **16a**−**f** and Celecoxib

	IC_{50}[a] (μM)		COX-2 inhibition (%)		
cmpd	COX-1	COX-2	10 μM	1 μM	selectivity index[b]
1a	>100	0.010	100	100	>10 000
1b	>100	0.020	100	87	>5000
1c	>100	0.026	90	87	>4000
1d	>100	0.010	100	91	>10 000
2a	>100	0.40	75	50	>250
2b	>100	5.40	62	35	>19
2c	>100	0.55	78	59	>200
2d	>100	ND[c]	27	0	
2e	>100	1.96	79	33	>50
2f	>100	ND	ND	ND	
12a	>100	11.0	51	19	>9
12b	>100	8.40	55	8	>12
12c	>100	0.94	70	59	>100
12d	>100	0.90	75	55	>100
16a	>100	ND	12	0	
16b	>100	ND	29	0	
16c	>100	ND	49	21	
16d	>100	ND	30	0	
16e	>100	ND	25	0	
16f	>100	ND	34	30	
celecoxib	3.7	0.06	100	80	61.7

[a] Results are expressed as the mean ($n = 3$) of the % inhibition of PGE_2 production by test compounds with respect to control samples. [b] In vitro COX-2 selectivity index ($IC_{50(COX-1)}/IC_{50(COX-2)}$). [c] ND: not determined.

COX-2, also retaining some COX-1/COX-2 selectivity. The marked difference in activity among the ester derivatives suggested the importance of the SO_2Me pharmacophoric portion in the phenyl ring when placed at C5 instead of N1. Furthermore, compounds **1a**−**d** showed inhibition values toward COX-2 (0.010, 0.020, 0.026, and 0.010 μM, respectively) higher than that of celecoxib (0.06 μM) or the previously described lead compound **7a** (0.04 μM). Similarly, COX-1/COX-2 selectivity was significantly improved in comparison to both **7a** and the reference compounds.

Analysis of the influence of substituents and substitution pattern on the activity and selectivity toward COX-2 showed that the presence and the position occupied by the fluorine atom at the N1 phenyl ring plays an important role in defining the inhibitory activity toward COX-2 in the in vitro cell culture assay. In particular, **1d**, bearing a fluorine atom at the meta position, was found to be the most active compound (0.010 μM). Moving the fluorine substituent to the *para*-position, as for **1a**, activity was maintained, while the simultaneous presence of two fluorine atoms at the meta and para positions (**1b**) led to a slight reduction of activity (0.020 μM) and selectivity. SAR data indicate that the SO_2Me at the C5 phenyl ring and a fluorine substituent at the N1 phenyl ring are cooperative determinants of both potent and selective COX-2 inhibition.

Compound **1d** was submitted to further pharmacological tests. In particular, the HWB assay was performed to predict the actual extent of isozyme inhibition achievable in vivo by circulating drug levels, because of a number of variables potentially affecting drug−enzyme interaction. Results indicated that, in these experimental conditions, the situation is reversed with celecoxib being more selective than compound **1d**. In fact, celecoxib showed a COX-1/COX-2 IC_{50} ratio of 23 in the HWB assay (Figure 1), whereas a COX-1/COX-2 IC_{50} ratio of 62 was found in cell culture assay. On the other hand, **1d** showed a 9.7 ratio in the HWB assay and a >10 000 ratio in cell culture assay. The discrepancy of these results could be due to different inhibitor sensitivities shown by the mouse and human COX isozymes, as reported for other anti-inflammatory compounds.[23]

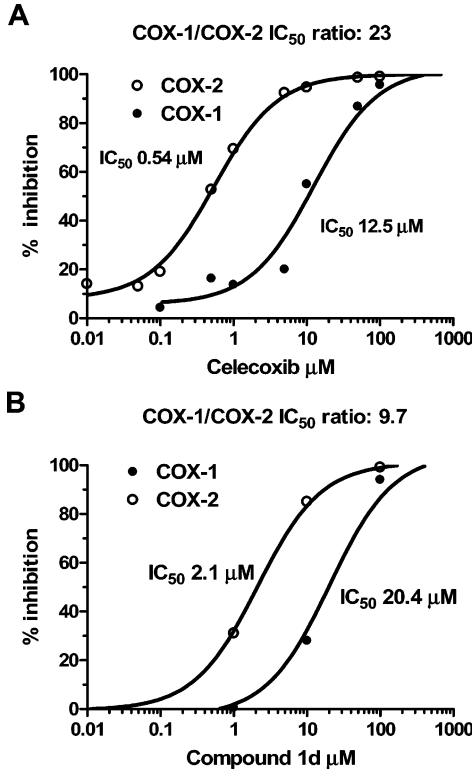

Figure 1. In vitro inhibition (whole blood assay) of COX-1 and COX-2 by celecoxib (A) and **1d** (B). Results are expressed as average percent inhibition of three donors of prostanoid production assessed in the absence of the test compounds (control). COX-2 selectivity index ($IC_{50(COX-1)}/IC_{50(COX-2)}$).

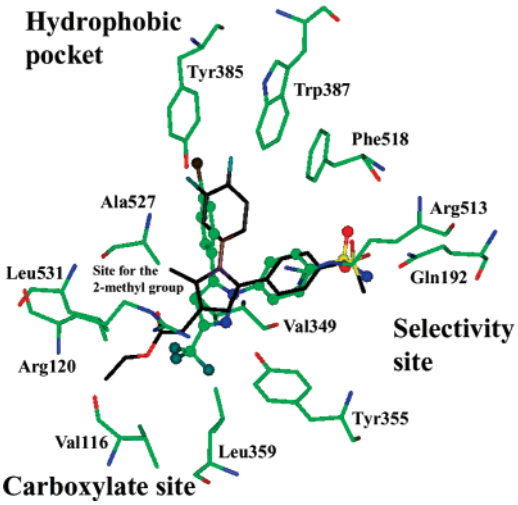

Figure 2. Graphical representation of the binding mode of **1b** (black) with respect to the cocrystallized inhibitor SC-558 (green, ball and stick notation). Portions of the binding site are labeled according to the notation of Kurumbail and co-workers.[26]

Finally, to assess in vivo anti-inflammatory and analgesic activity of **1d**, the rat paw pressure test, the paw volume test, and the abdominal constriction test were also performed (Tables 2−4). This compound, administered at a dose of 20 mg/kg p.o., showed a very good activity against carrageenan-induced hyperalgesia 30 min after administration. Such an analgesic activity at this time was very similar to that obtained with celecoxib (10 mg/kg p.o.). However, in contrast to what was observed with this standard compound, the activity tended to fade at longer time-points (1 h), disappearing almost completely 2 h after administration (Table 2). In parallel, a very good

Table 2. Effect of Compound **1d** in the Rat Paw-Pressure Test, in Comparison to Celecoxib[a]

		paw pressure (g)			
			after treatment		
pretreatment	treatment	before pretreatment	30 min	60 min	120 min
saline	saline	62.0 ± 4.3	62.6 ± 5.2	63.5 ± 4.6	64.2 ± 5.2
carrageenan	saline	61.9 ± 5.1	38.7 ± 5.3	35.8 ± 4.5	40.1 ± 5.0
carrageenan	**1d**	61.7 ± 3.9	55.2 ± 3.6	49.8 ± 4.1	43.4 ± 4.9
carrageenan	celecoxib	62.7 ± 3.9	56.5 ± 3.8	58.2 ± 4.4	55.2 ± 5.1

[a] Compound **1d** and celecoxib were administered, respectively, at the dose of 20 and 10 mg/kg.

Table 3. Effect of Compound **1d** in Comparison with Celecoxib in the Edema Induced by Carrageenan[a]

		paw volume (mL)		
pretreatment	treatment	before pre-treatment	60 min after treatment	% of paw-edema suppression
saline	saline	1.26 ± 0.09	1.31 ± 0.10	
carrageenan	saline	1.22 ± 0.08	2.33 ± 0.08	
carrageenan	**1d**	1.24 ± 0.11	1.29 ± 0.14	95.5
carrageenan	celecoxib	1.28 ± 0.14	1.33 ± 0.10	95.5

[a] Compound **1d** and celecoxib were administered, respectively, at the dose of 20 and 10 mg/kg.

Table 4. Effect of Compound **1d** in the Mouse Abdominal Constriction Test (0.6% Acetic Acid)

treatment[a]	number of mice	dose (p.o. mg·kg^{-1})	number of writhes
CMC	20		31.4 ± 4.3
1d	10	10	28.9 ± 23.9
1d	7	20	15.7 ± 3.6

[a] All compounds were administered per os 30 min before test. *P < 0.01 versus vehicle-treated mice.

activity was demonstrated against carrageenan-induced oedema in the rat paw (Table 3), with a complete remission 1 h after the administration (20 mg/kg p.o.). Moreover, a dose-dependent anti-nociceptive activity was observed in the abdominal constriction test (Table 4).

Molecular Modeling Simulations

In a previous work,[17] a series of 1,5-diarylpyrrole derivatives was submitted to a two-step computational protocol consisting of molecular docking calculations and structural optimization of the complexes obtained, with the aim of investigating on the possible interaction mode of such inhibitors within the COX-2 binding site. Moreover, Grid maps[25] were calculated for some probe atoms or groups to evaluate the regions of best interaction between the inhibitors and the macromolecule. As a result, in addition to findind for the inhibitors an orientation very similar to that of the cocrystallized ligand SC-558, molecular modeling simulations suggested structural modifications of the parent compounds to synthesize a second generation of pyrrole derivatives endowed with an improved biological profile. In particular, the analysis of the Grid map generated for the fluoride probe suggested that a fluorine substituent at the para positions of the pyrrole N1-phenyl ring (similar to the bromine atom of SC-558) and, additionally, at the meta position of the same ring, could improve the interaction with the COX-2 binding site, involving Trp387, Tyr348, and Tyr385 of the hydrophobic cavity. Accordingly, the three fluorinated derivatives **1a**, **1b**, and **1d** were found to have a very low IC_{50} toward COX-2 (up to a 10 nM concentration) with a selectivity index (expressed as the ratio between $IC_{50(COX-1)}/IC_{50(COX-2)}$) higher than 10 000, further validating the reliability of the computational protocol in finding the binding mode of 1,5-diaryl-2-methyl-3-substituted pyrrole derivatives within the COX-2 binding site.

The new derivatives were submitted to the same computational protocol previously reported, with the aim of analyzing their interactions with amino acids of the COX-2 binding site. In the complexes obtained, the diaryl system of compounds **1** was superposed on the corresponding structural feature of the cocrystallized inhibitor. In particular, the difluorophenyl ring at N1 of the pyrrole core of **1b** and the *p*-bromophenyl moiety of SC-558 were located in the hydrophobic pocket (according to the notation used by Kurumbail et al.)[26] and interacted with the side chains of hydrophobic (Leu384) and aromatic (Tyr385, Trp387, and Phe518) residues (Figure 2). As expected, fluorine substituents at the meta and para positions of the N1 phenyl ring lay on one of the best interaction regions of the fluoride Grid map. Moreover, the methyl group at the position 2 of the pyrrole ring provided profitable interactions with the hydrophobic side chains of Val349 and Ala527. This result was in agreement with the Grid map generated for the methyl probe, showing a profitable interaction point (at −3.0 kcal/mol) corresponding to the region occupied by the 2-methyl group of inhibitors, also in agreement with previous findings suggesting that such a substituent at this position leads to the optimal potency.[19] On the other hand, the ester moiety at position 3 of **1b** was superposed on the trifluoromethyl group of the cocrystallized inhibitor and was involved with its oxygen atoms in hydrogen bond contacts with the basic terminal group of the Arg120 side chain (belonging to the classical NSAID's carboxylate binding site), in agreement with the carbonyl Grid map showing that the Arg120 side chain was surrounded by regions of profitable interactions with a carbonyl group (at −7 kcal/mol), including the position occupied by the carbonyl ester group of **1b**. The alkyl portion of the ester group interacted with Val116 and Tyr355 and was directed toward the solvent accessible surface. Finally, the *p*-methylsulfonylphenyl moiety at the position 5 of **1b** occupied the same region of space as the *p*-sulfonamidophenyl substituent of SC-558, both of them being accommodated within the selectivity site. In this context, the entire *p*-methylsulfonylphenyl group of the inhibitor was involved in profitable interactions with COX-2 residues. In fact, the oxygen atoms of the sulfone groups showed hydrogen bond contacts with the terminal NH_2 group of Gln192 and with the backbone NH group of Phe518, while the aromatic ring interacted with the side chain of hydrophobic amino acids, such as Leu352 and Val523.

Inversion of the substitution pattern at positions 1 and 5 of the pyrrole ring of compounds **1** led to **2**, characterized by a marked decrease in activity toward COX-2 (up to 270-fold, compare **1b** vs **2b**), accounted for by a different interaction pathway with the enzyme, due to a reorientation of the inhibitors within the binding site. As an example, the first-ranked orientation of **2b**, while characterized by the usual orientation of the fluorophenyl moiety within the hydrophobic pocket,

showed the ester side chain anchored to the selectivity site by a hydrogen bond between the carbonyl oxygen and the NH group of Phe518 and by hydrophobic contacts involving the ethyl terminal group and a portion of the Gln192 side chain. On the other hand, the methyl group at the position 2 of the pyrrole ring was accommodated into a region defined by His90, Ser353, and Tyr355 without any profitable interaction, while the aromatic moiety at N1 was embedded into the carboxylate site. In particular, one of the sulfone oxygens interacted by a hydrogen bond the guanidino group of Arg120, and the terminal methyl group linked to the sulfur atom was allocated to a large hydrophobic region delimited by the side chains of Val116, Leu359, and Lue531. Although the best orientation of **2b** showed electrostatic and hydrophobic interactions contributing to the stabilization of the complex with COX-2, it lacked additional contacts found for **1b**, thus accounting for the marked decreased activity of **2b** with respect to **1b**. As examples, hydrogen bonds at both the carboxylate site (namely, with Arg120) and the selectivity site (namely, with Gln192) were omitted, as well as the hydrophobic interactions involving the 2-methyl group. Inspection of the various orientations/conformations found for **2b** during docking simulations led us to identify an orientation of the inhibitor, very similar to that of the best ranked orientation of **1b**. In fact, while substituents at positions 1, 3, and 5 of **2b** were isooriented with respect to the same substituents of **1b** (i.e., the methylsulfonylphenyl group into the selectivity site, the fluorophenyl moiety into the hydrophobic pocket, and the ester side chain into the carboxylate site), the methyl group at position 2 of **2b** pointed toward Tyr355 and, to avoid steric clashes with this residue, caused a translation of the molecule toward the hydrophobic pocket with a consequent lack of hydrogen bond contacts with Arg120. In summary, docking calculations showed that the most frequent orientations of **2b** within the binding site were all characterized by interaction pathways accounting for the lower activity of this compound with respect to the corresponding isomer **1b**.

Regarding keto-ester derivatives, the conformational rigidity introduced at the position 3 significantly influenced their binding mode into the binding site of COX-2. As an example, the best orientation of **12b** showed the methylsulfone group accommodated within the hydrophobic pocket, while the methyl group was in the carboxylate site. In such an orientation, although the ester carbonyl group of the inhibitor made the usual hydrogen bond with the NH of Phe518, the remaining interactions (i.e., the hydrogen bond involving Arg120 and the ester chain and the contacts with the hydrophobic pocket), important for a profitable binding within the active site, were lost. Considering the low affinity with respect to the corresponding ester derivatives (and consequent lower selectivity between the two forms of the enzyme), probably due to the different structural properties introduced into the side chain at the position 3 of the pyrrole nucleus, keto-esters were not considered attractive compounds and were not investigated further.

Conclusions

Based on suggestions derived from both SAR analysis and molecular modeling simulations on 1,5-diarylpyrrole derivatives, a new series of compounds has been designed and synthesized. Biological data showed a significant enhancement of their affinity toward COX-2 and an improvement of COX-2/COX-1 selectivity, with respect to the parent compounds in the in vitro cell culture assay.

One of the new entries (namely, **1d**) was selected for further in vitro and in vivo experiments. In the HWB assays, **1d** had a COX-1/COX-2 ratio lower than that of the reference drug celecoxib, but comparable to that of other NSAIDs, such as meloxicam.[27] The new compound showed a very interesting anti-inflammatory and analgesic activity, laying the foundations for developing new lead compounds that could be effective agents in the management of inflammation and pain.

Experimental Section

Chemistry. All chemicals used were of reagent grade. Yields refer to purified products and are not optimized. Melting points were determined in open capillaries on a Gallenkamp apparatus and are uncorrected. Microanalyses were carried out by means of a Perkin-Elmer 240C or a Perkin-Elmer Series II CHNS/O Analyzer 2400. Merck silica gel 60 (230−400 mesh) was used for column chromatography. Merck TLC plates, silica gel 60 F_{254} were used for TLC. ^{1}H NMR spectra were recorded with a Bruker AC 200 spectrometer in the indicated solvent (TMS as internal standard). The values of the chemical shifts are expressed in ppm and the coupling constants (*J*) in Hz. Mass spectra were recorded on either a Varian Saturn 3 or a ThermoFinnigan LCQ-deca spectrometer.

General Procedure for Preparation of Pentane-1,4-diones 9 and 14a−f. To a solution of the suitable benzaldehyde (12 mL, 0.09 mol) in ethanol (30 mL), triethylamine (19.5 mL, 0.14 mol), methyl vinyl ketone (5.8 mL, 0.07 mol), and 3-ethyl-5-(2-hydroxyethyl)-4-methylthiazolium bromide (3.53 g, 0.014 mol) were added. The mixture was heated at 75−80 °C for 20 h under nitrogen and then cooled. The solvent was removed under reduced pressure and the residue treated with 2 N HCl (300 mL). After extraction with dichloromethane, the organic layer was washed with aqueous $NaHCO_3$ and water. The organic fractions were dried over Na_2SO_4, filtered, and concentrated to give a crude orange liquid (16.2 g). After chromatography on silica gel (hexane/ethyl acetate, 7/3 v/v), the desired compounds **9** or **14a−f** were isolated (yield 70%) as a light yellow solid which, after recrystallization from hexane, gave an analytical sample as light yellow needles.

Examples. 1-[4-(Methylthio)phenyl]pentane-1,4-dione (9). Yellowish needles (yield 78%). Analytical data, mp, and ^{1}H NMR spectrum were consistent with those reported in the literature.[19]

1-[4-(3,4-Difluoro)phenyl]pentane-1,4-dione (14b). Yellowish needles (yield 78%), mp 57 °C; ^{1}H NMR ($CDCl_3$) 7.77 (m, 2H), 7.23 (m, 1H), 3.18 (t, $J = 6.7$ Hz, 2H), 2.88 (t, $J = 6.7$ Hz, 2H), 2.23 (s, 3H). Anal. ($C_{11}H_{10}O_2F_2$) C, H, O, F.

1-[4-(Methoxy)phenyl]pentane-1,4-dione (14c). Yellowish needles (yield 77%). Analytical data, mp, and ^{1}H NMR spectrum were consistent with those reported in the literature.[28]

1-[4-(Methylsulfonyl)phenyl]pentane-1,4-dione (10). To a solution of **9** (7.8 g, 35 mmol) in methanol (150 mL), oxone (37.7 g, 61.4 mmol), dissolved in water (150 mL), was added over 5 min. After stirring at 25 °C for 2 h, the reaction mixture was diluted with water (400 mL) and extracted with dichlorometane (3 × 400 mL). The organic layer was washed with brine (200 mL) and water (200 mL) and dried (Na_2SO_4). After filtration and concentration, the crude material was chromatographed (silica gel, hexane/ethyl acetate, 3/1) to give **10** (yield 90%) as a yellowish solid that, after recrystallization from hexane/ethyl acetate, gave an analytical sample as white needles. Analytical data, mp, and ^{1}H NMR spectrum were consistent with those reported in the literature.[19]

4-Methylsulfonylaniline. A mixture of Na_2WO_4 (0.067 g), 8 drops of acetic acid, and H_2O (19 mL) was placed in a flask and heated to 65 °C. 4-Methylthioaniline (19 mL, 153 mmol) was added, followed by dropwise addition of H_2O_2 (34.5 mL, 337 mmol). The mixture was stirred at 65 °C for 1.5 h and, after cooling, 800 mL of 1 N HCl and 500 mL of $CHCl_3$ were added. The layers were separated, and the aqueous phase was washed with additional $CHCl_3$. The aqueous phase was basified with 25% NaOH and extracted with $CHCl_3$. The organic phase was washed with brine and dried over Na_2SO_4. The solvent was removed to give 4-methylsulfonylaniline as a white solid. Analytical data, mp, and ^{1}H NMR spectrum were consistent with those reported in the literature.[22]

General Procedure for the Preparation of 1,5-Diarylpyrroles 11a−d and 15a−f. These compounds were prepared by means of the Paal−Knorr reaction by condensing a 1,4-diketone with the appropriate aniline. Briefly, a mixture of diketone **10** or **14a−f** (2.28 mmol) and the suitable aniline (2.5 mmol) in the presence of *p*-toluenesulfonic acid (30 mg) in dry toluene (50 mL) was refluxed for 20 h using a Dean−Stark apparatus. The reaction mixture was cooled, filtered, and concentrated. The crude material was purified by flash chromatography with a hexane/ethyl acetate (7/3 v/v) mixture as the eluent to give the expected 1,5-diarylpyrrole as a solid in satisfactory yield. Recrystallization from hexane/ethyl acetate gave the required product.

2-Methyl-5-[4-(methylsulfonyl)phenyl]-1-[4-(methoxy)phenyl]-1*H*-pyrrole (11c). White needles (yield 85%), mp 144 °C, ^{1}H NMR ($CDCl_3$) 7.67 (d, 2H, J = 7.27 Hz), 7.19 (d, 2H, J = 7.27 Hz), 7.07 (d, 2H, J = 7.27 Hz), 6.92 (d, 2H, J = 7.27 Hz), 6.50 (d, 1H, J = 3.5 Hz), 6.11 (d, 1H, J = 3.5 Hz), 3.84 (s, 3H), 3.00 (s, 3H), 2.12 (s, 3H). Anal. ($C_{19}H_{19}NO_3S$) C, H, N, O, S.

2-Methyl-1-[4-(methylsulfonyl)phenyl]-5-[4-(methoxy)phenyl]-1*H*-pyrrole (15c). Yellowish needles (yield 82%), mp 156 °C, ^{1}H NMR ($CDCl_3$) 7.93 (d, 2H, J = 7.27 Hz), 7.30 (d, 2H, J = 7.27 Hz), 6.93 (d, 2H, J = 7.27 Hz), 6.92 (d, 2H, J = 7.27 Hz), 6.27 (d, 1H, J = 3.5 Hz), 6.11 (d, 1H, J = 3.5 Hz), 3.75 (s, 3H), 3.09 (s, 3H), 2.17 (s, 3H). Anal. ($C_{19}H_{19}NO_3S$) C, H, N, O, S.

General Procedure for the Preparation of Ethyl 1,5-Diarylpyrrol-3-ylglyoxylic Esters 12a−d or 16a−f. These compounds were prepared by reaction of ethoxalyl chloride with the appropriate pyrrole in the presence of pyridine, as previously reported.[20] A solution of pyridine (11 mmol) in anhydrous dichloromethane was added to a stirred solution of ethoxalyl chloride (1.22 mL, 10 mmol) in dichloromethane (15 mL) at a rate that allowed the temperature to be maintained between −20 to −25 °C. Immediately after, a solution of the pyrrole derivative (10 mmol) in dichloromethane (15 mL) at the same temperature was added. The solution was stirred for 4 h at 0 °C, then washed in sequence with dilute HCl and saturated aqueous NaCl solution. The organic solution was dried and evaporated in vacuo. Purification of the residue by flash chromatography with ethyl acetate as the eluant gave a solid which, after recrystallization from hexane/ethyl acetate, afforded the expected product.

Ethyl-2-methyl−5-[4-(methylsulfonyl)phenyl]-1-[4-(fluoro)-phenyl]-1*H*-pyrrol-3-glyoxylate (12a). Yellowish needles (yield 82%), mp 146 °C, ^{1}H NMR ($CDCl_3$) 7.93 (m, 2H), 7.76 (m, 2H), 7.00 (m, 2H), 7.02 (m, 2H), 6.00 (s, 1H), 4.20 (q, 2H, J = 7.1 Hz), 2.86 (s, 3H), 2.16 (s, 3H), 1.30 (t, 3H, J = 7.1 Hz). Anal. ($C_{22}H_{20}NO_5SF$) C, H, N, S, O, F.

Ethyl-2-methyl−1-[4-(methylsulfonyl)phenyl]-5-[4-(fluoro)-phenyl]-1*H*-pyrrol-3-glyoxylate (16a). Yellowish needles (yield 75%), mp 187 °C, ^{1}H NMR ($CDCl_3$) 7.90 (m, 2H), 7.50 (m, 2H), 7.46 (m, 2H), 7.03 (m, 2H), 6.00 (s, 1H), 4.20 (q, 2H, J = 7.1 Hz), 2.86 (s, 3H), 2.16 (s, 3H), 1.30 (t, 3H, J = 7.1 Hz). Anal. ($C_{22}H_{20}NO_5S$) C, H, N, S, O, F.

1,5-Diarylpyrrole-3-acetic Esters 1a−d or 2a−f. These compounds were prepared by reduction of the appropriate glyoxylic derivative by means of triethylsilane in TFA[21] under a nitrogen atmosphere at 0 °C. To a solution of the suitable α-keto ester (2.3 mmol) in TFA (9 mL) stirred at 0 °C under nitrogen, triethylsilane (0.75 mL, 4.7 mmol) was slowly added, and the mixture was stirred for 30 min at rt. At the end of the reaction, the mixture was made alkaline with 40% aqueous ammonia (10 mL) and extracted with $CHCl_3$ (250 mL). The organic solution was dried and evaporated in vacuo. The resulting residue was chromatographed on silica gel eluting with $CHCl_3$ to give a solid which, after recrystallization from hexane/ethyl acetate, afforded the desired product.

Ethyl-2-methyl−5-[4-(methylsulfonyl)phenyl]-1-[4-(fluoro)-phenyl]-1*H*-pyrrol-3-acetate (1a). Yellowish needles (yield 71%), mp 133 °C, ^{1}H NMR ($CDCl_3$) 7.99 (m, 2H), 7.76 (m, 2H), 7.20 (m, 2H), 7.00 (m, 2H), 5.80 (s, 1H), 4.12 (q, 2H, J = 7.1 Hz), 3.39 (s, 2H), 2.84 (s, 3H), 2.16 (s, 3H), 1.30 (t, 3H, J = 7.1 Hz). Anal. ($C_{22}H_{22}NO_4SF$) C, H, N, S, O, F.

Ethyl-2-Methyl−1-[4-(methylsulfonyl)phenyl]-5-[4-(fluoro)-phenyl]-1*H*-pyrrol-3-acetate (2a). Yellowish needles (yield 65%), mp 144 °C, ^{1}H NMR ($CDCl_3$) 7.92 (m, 2H), 7.50 (m, 2H), 7.46 (m, 2H), 7.03 (m, 2H), 5.80 (s, 1H), 4.12 (q, 2H, J = 7.1 Hz), 3.39 (s, 2H), 2.82 (s, 3H), 2.12 (s, 3H), 1.33 (t, 3H, J = 7.1 Hz). Anal. ($C_{22}H_{22}NO_4SF$) C, H, N, S, O, F.

Biology. Arachidonic acid was obtained from SPIBIO (Paris, France). [^{3}H]-PGE_2 and [^{3}H]-TXB_2 were from Perkin-Elmer Life Sciences (Milan, Italy). All other reagents and compounds used were obtained from Sigma-Aldrich (Milan, Italy).

Cellular Assay. Cell Culture. The murine monocyte/macrophage J774 cell line was grown in Dulbecco's modified Eagles medium (DMEM) supplemented with 2 mM glutamine, 25 mM Hepes, penicillin (100 U/mL), streptomycin (100 μg/mL), 10% foetal bovine serum (FBS), and 1.2% sodium pyruvate (Bio Whittaker, Europe). Cells were plated in 24-well culture plates at a density of 2.5×10^5 cells/mL or in 10 cm-diameter culture dishes (1×10^7 cells/10 mL/dish) and allowed to adhere at 37 °C in 5% CO_2/95% O_2 for 2 h. Immediately before the experiments, the culture medium was replaced by a fresh medium without FBS to avoid interference with radioimmunoassay,[29] and cells were stimulated as described.

Assessment of COX-1 Activity. Cells were pretreated with the reference standard or the test compounds (0.01−10 μM) for 15 min and further incubated at 37 °C for 30 min with 15 μM arachidonic acid to activate the constitutive COX.[28] Stock solutions of the reference standard or of the test compounds were prepared in dimethyl sulfoxide (DMSO), and an equivalent amount of DMSO was included in control samples. At the end of the incubation, the supernatants were collected for the measurement of PGE_2 by radioimmunoassay.

Assessment of COX-2 Activity. Cells were stimulated for 24 h with *E. coli* lipopolysaccharide (LPS, 10 μg/mL) to induce COX-2, in the absence or presence of test compounds, at the concentrations previously reported. The supernatants were collected for the measurement of PGE_2 by radioimmunoassay.

Human Whole Blood (HWB) Assay. Subjects. Three healthy volunteers (2 females and 1 male, aged 29 ± 3 years) were enrolled to participate in the study after its approval by the Ethical Committee of the University of Chieti. Informed consent was obtained from each subject.

COX-2 Assay. To evaluate COX-2 activity, 1 mL aliquots of peripheral venous blood samples containing 10 i.u. of sodium heparin were incubated in the presence of LPS (10 μg/mL) or saline for 24 h at 37 °C, as previously described.[23] The contribution of platelet COX-1 was suppressed by pretreating the subjects with aspirin (300 mg, 48 h) before sampling. Plasma was separated by centrifugation (10 min at 2000 rpm) and kept at −80 °C until assayed for PGE_2, as an index of LPS-induced monocyte COX-2 activity.

COX-1 Assay. Peripheral venous blood samples were drawn from the same donors when they had not taken any NSAID during the 2 weeks preceding the study. Aliquots (1 mL) of whole blood were immediately transferred into glass tubes and allowed to clot at 37 °C for 1 h. Serum was separated by centrifugation (10 min at 3000 rpm) and kept at −80 °C until assayed for TXB_2. Whole blood TXB_2 production was measured as a reflection of maximally stimulated platelet COX-1 activity in response to endogenously formed thrombin.[24]

Effects of COX-2 Inhibitors on Whole Blood COX-2 and COX-1 Activities. Celecoxib (0.005−50 mM) and **1d** (0.5−50 mM) were dissolved in DMSO. Aliquots of the solutions (2 μL) were pipetted directly into test tubes to give final concentrations of 0.01−100 μM in heparinized whole blood samples in the presence of LPS (10 μg/mL) for 24 h or with whole blood samples allowed to clot at 37 °C for 1 h to examine the concentration-dependence of COX-2 versus COX-1 inhibition, respectively.

Analysis of PGE_2 and TXB_2. PGE_2 and TXB_2 concentrations were measured by previously described and validated radioimmunoassays.[23,24] Unextracted plasma and serum samples were diluted in the standard diluent of the assay (0.02 M phosphate buffer, pH

7.4) and assayed in a volume of 1.5 mL at a final dilution of 1:50−1:30 000. [^{3}H]PGE_2 or [^{3}H]TXB_2 (4000 dpm, specific activity > 100 Ci/mmol, 1:100 000 dilution) and anti-TXB_2 (1:120 000 dilution) sera were used. The least detectable concentration was 1−2 pg/mL for both prostanoids.

Statistical Analysis. Results are expressed as the mean, for three experiments (triplicate wells were used for the various conditions of treatment, in the cell culture assay) of the percent inhibition of prostanoid production assessed in the absence of the test compounds (control). Concentration−response curves were fitted, and IC_{50} values were analyzed with PRISM (GraphPad, San Diego, CA) and ALLFIT, a basic computer program for simultaneous curve-fitting based on a four-parameter logistic equation.

In Vivo Anti-Inflammatory Activity. Animals. Male Swiss albino mice (23−25 g) and Sprague−Dawley or Wistar rats (150−200 g) were used. Fifteen mice and four rats were housed per cage. The cages were placed in the experimental room 24 h before the test for acclimatization. The animals were fed in a standard laboratory diet and tap water ad libitum and kept at 23 ± 1 °C with a 12 h light/dark cycle, light on at 7 a.m. All experiments were carried out in accordance with the NIH Guide for the Care and Use of Laboratory animals. All efforts were made to minimize animal suffering, and to reduce the number of animals used.

Paw Pressure Test. The nociceptive threshold in the rat was determined with an analgesimeter, according to the method described by Leighton.[30] Threshold pressure was measured before and 30, 60, and 120 min after treatment. An arbitrary cutoff value of 250 g was adopted. To induce an inflammatory process in the rat, paw carrageenan (0.1 mL, 1%) was administered i.pl. 4 h before test.

Carrageenan-Induced Paw Edema. Rat paw volumes were measured using a plethysmometer. Five hours after the injection of carrageenan (0.1 mL injection of 1.0%) the paw volume of the right hind paw was measured and compared with saline/carrageenan-treated controls.[31] Rats received test compounds 4 h after carrageenan. Results are reported as paw volume expressed in mL.

Abdominal Constriction Test. Mice were injected i.p. with a 0.6% solution of acetic acid (10 mL/kg), according to Koster.[32] The number of stretching movements was counted for 10 min, starting 5 min after acetic acid injection.

Computational Details. All calculations and graphical manipulations were performed on Silicon Graphics computers (Origin 300 server and Octane workstations) using the software package Autodock 3.0.5[33] and MacroModel 8.5.[34]

Atomic coordinates of COX-2 used during molecular modeling simulations were derived from the structure of the complex between COX-2 and SC-558 (**3a**, Chart 1), refined at a 3 Å resolution (Brookhaven Protein Data Bank entry: 6cox). To set the initial coordinates for the docking studies, the residues belonging to chain B and three *N*-acetyl-D-glucosamine residues present in chain A of the crystal structure of COX-2 were removed and excluded from all calculations.

The program Autodock was used to evaluate the binding mode of the new inhibitors and to explore their binding conformations within the COX-2 structure. A grid point spacing of 0.28 Å and 87 × 81 × 97 points were used. The grid was centered on the mass center of the crystallographic inhibitor. Parameters for docking runs were set as follows (imported from a docking parameter file): outlev 1, diagnostic output level; rmstol 0.5, cluster_tolerance/A; extnrg 1000.0, external grid energy; e0max 0.0 10000, max initial energy; max number of retries; ga_pop_size 50, number of individuals in population; ga_num_evals 250000, maximum number of energy evaluations; ga_num_generations 27000, maximum number of generations; ga_elitism 1, number of top individuals to survive to next generation; ga_mutation_rate 0.02, rate of gene mutation; ga_crossover_rate 0.8, rate of crossover; ga_window_size 10; ga_cauchy_alpha 0.0, Alpha parameter of Cauchy distribution; ga_cauchy_beta 1.0, Beta parameter Cauchy distribution; set_ga, set the above parameters for GA or LGA; sw_max_its 300, iterations of Solis & Wets local search; sw_max_succ 4, consecutive successes before changing rho; sw_max_fail 4, consecutive failures before changing rho; sw_rho 1.0, size of local search space to sample; sw_lb_rho 0.01, lower bound on rho; ls_search_freq 0.06, probability of performing local search on individual; set_psw1, set the above pseudo-Solis & Wets parameters; ga_run 100, do this many hybrid GA-LS runs; analysis, perform a ranked cluster analysis.

Based on the fact that Autodock does not perform any structural optimization and energy minimization of the complexes found, a molecular mechanics/energy minimization (MM/EM) approach was applied to refine the Autodock output. The computational protocol applied consisted in the application of 10 000 steps of the steepest descent algorithm or until the derivative convergence was 0.01 kcal/Å·mol. Moreover, because of the large number of atoms in the model, to correctly optimize the COX-2−inhibitor complexes obtained by the flexible docking, the following additional constraints had to be imposed: (*i*) a subset, comprising only of the inhibitor and a shell of residues possessing at least one atom at a distance of 5 Å from any of the inhibitor atoms, was created and subjected to energy minimization. The inhibitor and all the amino acid side chains of the shell were unconstrained during energy minimization to allow for reorientation and proper hydrogen-bonding geometries and van der Waals contacts; (*ii*) all the atoms not included in the above-defined subset were fixed, but their nonbond interactions with all the relaxing atoms were calculated. Further details on this computational protocol have been reported elsewhere.[17]

Acknowledgment. Thanks are due to Italian MIUR for financial support.

Supporting Information Available: Experimental details of the synthesis, spectral data, and elemental analysis data of some representative compounds. This material is available free of charge via the Internet at http://pubs.acs.org.

References

(1) McGettigan, P.; Henry, D. Current Problems with Non-Specific COX Inhibitors. *Curr. Pharm. Des.* **2000**, *6*, 1693−1724.
(2) Kauffman, G. Aspirin-Induced Gastric Mucosal Injury: Lessons Learned from Animal Models. *Gastroenterology* **1989**, *96S*, 606−614.
(3) DeWitt, D. L. COX-2-Selective Inhibitors: The New Super Aspirins. *Mol. Pharm.* **1999**, *55*, 625−631.
(4) Moore, B. C.; Simmons, D. L. COX-2 Inhibition, Apoptosis, and Chemoprevention by Nonsteroidal Anti-Inflammatory Drugs. *Curr. Med. Chem.* **2000**, *7*, 1131−1144.
(5) Penning, T. D.; Tally, J. J.; Bertenshaw, S. R.; Carter, J. S.; Collins, P. W.; Doctor, S.; Graneto, M. J.; Lee, L. F.; Malecha, J. W.; Miyashiro, J. M.; Rogers, R. S.; Rogier, D. J.; Yu, S. S.; Anderson, G. D.; Burton, E. G.; Cogburn, J. N.; Gregory, S. A.; Koboldt, C. M.; Perkins, W. E.; Seibert, K.; Veenhuizen, A. W.; Zhang, Y. Y.; Isakson, P. C. Synthesis and Biological Evaluation of the 1,5-Diarylpyrazole Class of Cyclooxygenase-2 Inhibitors: Identification of 4-[5-(4-Methylphenyl)-3-(trifluoromethyl)-1*H*-pyrazol-1-yl]benzenesulfonamide (SC-58635, Celecoxib). *J. Med. Chem.* **1997**, *40*, 1347−1365.
(6) Prasit, P.; Wang, Z.; Brideau, C.; Chan, C. C.; Charleson, S.; Cromlish, W.; Ethier, D.; Evans, J. F.; Ford-Hutchinson, A. W.; Gauthier, J. Y.; Gordon, R.; Guay, J.; Gresser, M.; Kargman, S.; Kennedy, B.; Leblanc, Y.; Leger, S.; Mancini, J.; O'Neill, G. P.; Quellet, M.; Percival, M. D.; Perrier, H.; Riendeau, D.; Rodger, I.; Tagari, P.; Therien, M.; Vickers, P.; Wong, E.; Xu, L. J.; Young, R. N.; Zamboni, R.; Boyce, S.; Rupniak, N.; Forrest, M.; Visco, D.; Patrick, D. The Discovery of Rofecoxib [MK 966, Vioxx, 4-(4′-Methylsulfonylphenyl)-3-phenyl-2(5*H*)-furanone], an Orally Active Cyclooxygenase-2 Inhibitor. *Bioorg. Med. Chem. Lett.* **1999**, *9*, 1773−1778.
(7) Talley, J. A; Brown, D. L.; Carter, J. S.; Masferrer, M. J.; Perkins, W. E.; Rogers, R. S.; Shaffer, A. F.; Zhang, Y. Y.; Zweifel, B. S.; Seiberk, K. 4-[5-Methyl-3-phenylisoxazol-4-yl]-benzenesulfonamide, Valdecoxib: A Potent and Selective Inhibitor of COX-2. *J. Med. Chem.* **2000**, *43*, 775−777.
(8) Riendeau, D.; Percival, M. D.; Brideau, C.; Charleson, S.; Dube, D.; Ethier, D.; Falgueyret, J.-P.; Friesen, R. W.; Gordon, R.; Greig, G.; Guay, I.; Manacini, J.; Ouellet, M.; Wong, E.; Xu, L.; Boyce, S.; Visco, D.; Girad, Y.; Prasit, P.; Zamboni, R.; Rodger, J. W.;

Gresser, M.; Ford-Hutchinson, A. W.; Young, R. N.; Chan, C.-C. Etoricoxib (MK-0663): Preclinical Profile and Comparison with Other Agents That Selectively Inhibit Cyclooxygenase-2. *J. Pharmacol. Exp. Ther.* **2001**, *296*, 558−566.

(9) Davies, I. W.; Marcoux, J.-F.; Corley, E. G.; Journet, M.; Cai, D.-W.; Palucki, M.; Wu, J.; Larsen, R. D.; Rossen, K.; Pye, P. J.; Dimichele, L.; Dormer, P.; Reider, P. J. A Practical Synthesis of a COX-2-Specific Inhibitor. *J. Org. Chem.* **2000**, *65*, 8415−8420.

(10) Talley, J. Selective Inhibitors of Cyclooxygenase-2 (COX-2). *Prog. Med. Chem.* **1999**, *36*, 201−234.

(11) Scheen, A. J. Withdrawal of Rofecoxib (Vioxx): What About Cardiovascular Safety of COX-2-Selective Non-Steroidal Anti-Inflammatory Drugs? *Rev. Med. Liege* **2004**, *59*, 565−569.

(12) Kearney, P. M.; Baigent, C.; Godwin, J.; Halls, H.; Emberson, J. R.; Patrono, C. Do Selective Cyclooxygenase-2 Inhibitors and Traditional Non-Steroidal Anti-Inflammatory Drugs Increase the Risk of Atherothrombosis? Meta-Analysis of Randomised Trials. *Br. Med. J.* **2006**, *332*, 1302−1308.

(13) Chen, L. C.; Ashcroft, D. M. Risk of Myocardial Infarction Associated with Selective COX-2 Inhibitors: Meta-Analysis of Randomised Controlled Trials. *Pharmacoepidemiol. Drug Saf.* **2007**, *16*, 762−772.

(14) Rodriquez, L. A.; Patrignani, P. The Ever Growing Story of Cyclooxygenase Inhibition. *Lancet* **2006**, *368*, 1745−1747.

(15) Grosser, T.; Fries, S.; FitzGerald, G. A. Biological Basis for the Cardiovascular Consequences of COX-2 Inhibition: Therapeutic Challenges and Opportunities. *J. Clin. Invest.* **2006**, *116*, 4−15.

(16) Fries, S.; Grosser, T.; Price, T. S.; Lawson, J. A.; Kapoor, S.; DeMarco, S.; Pletcher, M. T.; Wiltshire, T.; FitzGerald, G. A. Marked Interindividual Variability in the Response to Selective Inhibitors of Cyclooxygenase-2. *Gastroenterology* **2006**, *130*, 55−64.

(17) Biava, M.; Porretta, G. C.; Cappelli, A.; Vomero, S.; Botta, M.; Manetti, F.; Giorni, G.; Sautebin, L.; Rossi, A.; Makovec, F.; Anzini, M. 1,5-Diarylpyrrole-3-acetic Acids and Esters as Novel Classes of Potent and Selective COX-2 Inhibitors. *J. Med. Chem.* **2005**, *48*, 3428−3432.

(18) Stetter, H. Catalyzed Addiction of Aldehydes to Activated Double Bonds—A New Synthetic Approach. *Angew. Chem., Int. Ed. Engl.* **1976**, *15*, 639−712.

(19) Khanna, I. K.; Weier, R. M.; Paul, Y. Y.; Collins, W.; Miyashiro, J. M.; Koboldt, C. M.; Veenhuizen, A. W.; Currie, J. L.; Seibert, K.; Isakson, P. C. 1,2-Diarylpyrroles as Potent and Selective Inhibitors of Cyclooxygenase-2. *J. Med. Chem.* **1997**, *40*, 1619−1633.

(20) Garofalo, A.; Corelli, F.; Campiani, G.; Bechelli, S.; Becherucci, C.; Tafi, A.; Nacci, V. Synthesis and Biological Evaluation of Conformationally Restricted Analogs of Tolmetin and Ketorolac. *Med. Chem. Res.* **1994**, *4*, 385−395.

(21) Anzini, M.; Canullo, L.; Braile, C.; Cappelli, A.; Gallelli, A.; Vomero, S.; Menziani, M. C.; De Benedetti, P. G.; Rizzo, M.; Collina, S.; Azzolina, O.; Sbacchi M.; Ghelardini, C.; Galeotti, N. Synthesis, Biological Evaluation, and Receptor Docking Simulations of 2-[(Acylamino)ethyl]-1,4-benzodiazepines as κ-Opioid Receptor Agonists Endowed with Antinociceptive and Antiamnesic Activity. *J. Med. Chem.* **2003**, *46*, 3853−3864.

(22) Almansa, C.; Alfón, J.; de Arriba, A. F.; Cavalcanti, F. L.; Escamilla, I.; Gómez, L. A.; Miralles, A.; Soliva, R.; Bartrolí, J.; Carceller, E.; Merlos, M.; García-Rafanell, J. Synthesis and Structure−Activity Relationship of a New Series of COX-2 Selective Inhibitors: 1,5-Diarylimidazoles. *J. Med. Chem.* **2003**, *46*, 3463−3475.

(23) Patrignani, P.; Panara, M. R.; Greco, A.; Fusco, O.; Natoli, C.; Iacobelli, S.; Cipollone, F.; Ganci, A.; Crèminon, C.; Maclouf, J.; Patrono, C. Biochemical and Pharmacological Characterization of the Cyclooxygenase Activity of Human Blood Prostaglandin Endoperoxide Synthases. *J. Pharmacol. Exp. Ther.* **1994**, *271*, 1705−1712.

(24) Patrono, C.; Ciabattoni, G.; Pinca, E.; Pugliese, F.; Castrucci, G.; De Salvo, A.; Satta, M. A.; Peskar, B. A. Low Dose Aspirin and Inhibition of Thromboxane B_2 Production in Healthy Subjects. *Thromb. Res.* **1980**, *17*, 317−327.

(25) *Grid*, version 21; Molecular Discovery, Ltd.: Marsh Road, Pinner, Middlesex, U.K.

(26) Kurumbail, R. G.; Stevens, A. M.; Gierse, J. K.; McDonald, J. J.; Stegeman, R. A.; Pak, J. Y.; Gildehaus, D.; Miyashiro, J. M.; Penning, T. D.; Seibert, K.; Isakson, P. C.; Stallings, W. C. Structural Basis for Selective Inhibition of Cyclooxygenase-2 by Anti-Inflammatory Agents. *Nature* **1996**, *384*, 644−648.

(27) Panara, M. R.; Renda, G.; Sciulli, M. G.; Santini, G.; Di Giamberardino, M.; Rotondo, M. T.; Tacconelli, S.; Seta, F.; Patrono, C.; Patrignani, P. Dose-Dependent Inhibition of Platelet Cyclooxygenase-1 and Monocyte Cyclooxygenase-2 by Meloxicam in Healthy Subjects. *J. Pharmacol. Exp. Ther.* **1999**, *290*, 276−280.

(28) Xue, S.; Li, L.-Z.; Liu, Y.-K.; Guo, Q.-X. Zinc-Mediated Chain Extension Reaction of 1,3-Diketones to 1,4-Diketones and Diastereoselective Synthesis of trans-1,2-Disubstituted Cyclopropanols *J. Org. Chem.* **2006**, *71*, 215−218.

(29) Zingarelli, B.; Southan, G. J.; Gilad, E.; O'Connor, M.; Salzman, A. L.; Szabò, C. The Inibitory Effects of Mercaptoalkylguanidines on Cyclooxygenase Activity. *Br. J. Pharmacol.* **1997**, *120*, 357−366.

(30) Leighton, G. E.; Rodriguez, R. E.; Hill, R. G.; Hughes, J. κ-Opioid Agonists Produce Antinociception after i.v. and i.c.v. but not Intrathecal Administration in the Rat. *Br. J. Pharmacol.* **1988**, *93*, 553−560.

(31) Sluka, A. K.; Westlund, K. N. Behavioral and Immunohistochemical Changes in an Experimental Arthritis Model in Rats. *Pain* **1993**, *55*, 367−377.

(32) Koster, R., Anderson, M.; de Beer, E. J. Acetic Acid for Analgesic Screening. *Fed. Proc.* **1959**, *18*, 412−418.

(33) Morris, G. M.; Goodsell, D. S.; Halliday, R. S.; Huey, R.; Hart, W. E.; Belew, R. K.; Olson, A. J. Automated Docking Using a Lamarckian Genetic Algorithm and and Empirical Binding Free Energy Function. *J. Comput. Chem.* **1998**, *19*, 1639−1662.

(34) Mohamadi, F.; Richards, N. G. J.; Guida, W. C.; Liskamp, R.; Lipton, M.; Caufield, C.; Chang, G.; Hendrickson, T.; Still, W. C. Macromodel—An Integrated Software System for Modeling Organic and Bioorganic Molecules Using Molecular Mehanics. *J. Comput. Chem.* **1990**, *11*, 440−467.

JM0707525